The effect and mechanism of Huangqin-Baishao herb pair in the treatment of dextran sulfate sodium-induced ulcerative colitis

Bailu Duan [a,b], Qiong Hu [c], Fengmin Ding [b], Fang Huang [b], Wei Wang [a,d], Nina Yin [b], Zhe Liu [a,b], Song Zhang [a], Dongchu He [a,**], Qiping Lu [a,e,*]

[a] Postdoctoral Research Station, General Hospital of Central Theater Command of PLA, Wuhan, 430070, China
[b] College of Basic Medicine, Hubei University of Chinese Medicine, Wuhan, 430065, China
[c] First People's Hospital of Jiangxia District, Wuhan City & Union Jiangnan Hospital, HUST, Wuhan, 430200, China
[d] Department of Orthopedics, Hubei Provincial Hospital of TCM Affiliated to Hubei University of Chinese Medicine, Wuhan, 430061, China
[e] Department of General Surgery, General Hospital of Central Theater Command of PLA, Wuhan, 430070, China

ARTICLE INFO

ABSTRACT

Background: The haungqing (*Scutellariae Radix*) and baishao (*Paeoniae Radix Alba*) herb pair (HBHP) is a common prescribed herbal formula or is added to other traditional Chinese medicine (TCM) prescriptions to treat ulcerative colitis (UC). However, the underlying mechanism is unclear.
Purpose: Elucidate the efficacy and potential mechanism of HBHP against UC.
Methods: First, The UC model of mice induced by dextran sulfate sodium (DSS) was established. The mice were randomly divided into Control group, DSS group, SASP group (390 mg/kg), and HPHP group (1.95 g/kg), with 8 mice per group. Drugs were administrated via oral gavage for 7 days. Then, Disease activity index (DAI), length of the colon, histopathology, and changes in inflammatory cytokines in colonic tissues were analyzed to assess the effect of HBHP on UC. Besides, Network pharmacology was applied to identify the active compounds, core targets of HBHP in the treatment of UC, and the corresponding signaling pathways to explore the underlying mechanisms. Finally, Western blot (WB), immunohistochemistry (IHC) and molecular docking were performed to validate the results.
Results: HBHP significantly reduced DAI score and decreased colon length shortening in DSS-induced UC mice. The administration of HBHP was able to effectively alleviated mucosal ulceration and epithelial destruction. In addition, HBHP treatment obviously - reduced the expressions of TNF-α, IL-6, and IL-1β in colon tissues ($p < 0.05$ or $p < 0.01$). 35 bioactive compounds and 290 HBHP targets related to UC were obtained. Among them 3 key active compounds (baicalein, panicolin, and norwogonin) with higher degree values in the drug-compound-target network and 21 hub genes (STAT3, JAK2, SRC, AKT1, PIK3CA, and VEGFA, etc.) were identified. KEGG enrichment analysis suggested that HBHP's mechanisms mainly involve the JAK-STAT pathway. Abnormal activation of JAK/STAT signaling is believed to be involved in the pathogeneses of UC. Notably, WB and IHC showed that HBHP significantly down-regulated the protein expression levels of p-JAK2 ($p < 0.05$) and p-STAT3 ($p < 0.05$ or $p < 0.01$). JAK2 and STAT3 might be core targets for the action of HBHP; this possibility was also supported by molecular docking.

* Corresponding author. Postdoctoral Research Station, General Hospital of Central Theater Command of PLA, Wuhan, 430070, China.
** Corresponding author.
E-mail addresses: hdc98@sina.com (D. He), ptwklqp111@163.com (Q. Lu).

Conclusions: HBHP could alleviate DSS-induced UC, reduce tissue inflammation, and its mechanism might primarily be achieved by inhibiting JAK2/STAT3 signaling pathway. Meanwhile, our work revealed that network pharmacology combined with experimental verification is a cogent means of studying the mechanism of TCM.

1. Introduction

Ulcerative colitis (UC) is a common chronic inflammatory bowel disease that primarily affect the mucosa and submucosa of the colon [1]. Importantly, the incidence of UC is increasing yearly worldwide [2] and the prevalence rate is projected to be 1 % among western populations by 2030 [3,4]. At present, although some therapeutic drugs, such as 5-aminosalicylic acid and glucocorticoids, can be used to treat UC, there still exist some adverse side-effects including drug dependence, drug resistance, hepatic and renal toxicity, etc [5–7]. Therefore, it is particularly important to seek and research new effective therapeutic drugs with less adverse effects for UC.

UC falls under the category of "dysentery", "diarrhea" and "hematochezia" in traditional Chinese medicine (TCM) [8]. As a sort of alternative and systematic complementary medicine with fewer adverse effects, TCM has gradually been recognized and accepted by more and more people around the world. The haungqin-baishao herb pair (HBHP) is a famous formula originated from Huangqin decoction, a classic TCM formula consisting of four herbs—Scutellariae Radix (Chinese name, Huangqin), Glycyrrhiza glabra L. (Chinese name, Gancao), Paeoniae Radix Alba (Chinese name, Baishao), and Jujubae Fructus (Chinese name, Daozao), recorded in the ancient book "Shang Han Lun" by Zhongjing Zhang in Eastern Han Dynasty, which is called "the ancestor of treating dysentery in all ages". In the formula, the "monarch herb" Huangqin is bitter and cold, clears heat, reduces turbidity, and stops dysentery; the "minister herb" Baishao is sour and cold, nourishes blood and astringes yin, and relieves pain; the auxiliary herbs Gancao and Daozao relieve pain. As the core components of this prescription, HBHP has been frequently used clinically in the treatment of UC, either alone or added to other TCM prescriptions. However, the pharmacological and molecular mechanisms of HBHP against UC remain unclear, which needs to be further studied.

TCM formulas typically incorporate multi-components and multiple targets for synergistic therapeutic effects [9], which is in line with the concept of network pharmacology analysis [10]. Network pharmacology based on polypharmacology, systems biology, and molecular networks [11], has shifted the paradigm of "one target, one drug" to the "multi-component-therapeutics, network-target" strategy, which is more effective for revealing the regulation principles of molecules in a high-throughput manner [12] and is well suited to study multitarget drug therapy and complex mechanisms of Chinese herbs [13].

In this study, the anti-UC effect of HBHP was investigated using a DSS-induced mouse model. Then, its underlying mechanism was predicted using network pharmacology and verified by Western blot, immunohistochemistry and molecular docking. Therefore, the aim of our study is to explore the efficacy and potential mechanism of HBHP against UC, so as to provide a theoretical basis for the clinical treatment of UC with HBHP.

2. Materials and methods

2.1. Animals and drugs

Male C57BL/6 J mice (21−25 g) were purchased from Liaoning Changsheng biotechnology co., Ltd. All mice were housed in a specific pathogen-free environment of 12/12-h light/dark cycles (lights off at 20:00), temperature $22 \pm 2\,°C$, and relative humidity (55 ± 5 %) in the experimental animal center of General Hospital of Central Theater Command of PLA (Wuhan, China). All mice could freely access to water and food in clear cages. In this study, experimental animal procedures were performed in strict accordance with international guidelines for care and use of laboratory animals and were approved by the Animal Ethics Committee of General Hospital of Central Theater Command of PLA (approval No. 2022202). Huangqin and baishao granules were purchased from Jiangyin Tianjiang Pharmaceutical Co., Ltd (Jiangyin, China). HBHP was obtained by mixing haungqin granule and baishao granule at a ratio of 3: 2 (w/w). Sulfasalazine (SASP) tablets were purchased from Shanghai Xinyi Tianping Pharmaceutical Co., Ltd (Shanghai, China).

2.2. Induction of UC model and treatment

UC was induced in mice by administration of 3.5 % (w/v) DSS (MP Biomedicals, MW 36–50 kDa) in drinking water for 7 days ad libitum as described previously [14]. Mice were randomly divided into four groups (n = 8 each): Control group (normal drinking water + normal water orally once daily), DSS group (DSS drinking water + normal water orally once daily), SASP group (DSS drinking water + 390 mg/kg SASP orally once daily), and HPHP group (DSS drinking water + 1.95 g/kg HBHP orally once daily). The dosage of HBHP used here was calculated in proportion to human clinical doses (15 g/day per adult) using body surface area conversion.

DSS solution was updated every day. The oral gavage administration was initiated simultaneously with DSS drinking water. Body weights, stool properties, and stool occult blood were monitored every day. At the end of the experiment, all mice were sacrificed and colonic specimens were collected. The lengths of the colons were measured and then immediately stored at $-80\,°C$ or fixed in 10 % paraformaldehyde for further procedures.

Table 1
Scoring system for DAI.

Sore	Weight loss	Stool consistency	Gross bleeding
0	None	Normal	Normal
1	1–5%	–	–
2	5–10 %	Loose stool	Hemoccult
3	10–15 %	–	–
4	>15 %	Diarrhea	Gross bleeding

2.3. Disease activity index (DAI)

DAI was measured and recorded according to a previous scoring system shown in Table 1 described by Zhuang HD et al. [15]. Occult blood was assessed using a fecal occult blood test kit (Mlbio, shanghai, China) and a blind method. DAI score was calculated using the formula: DAI = [(weight loss score) + (fecal character score) + (blood stool fraction)]/3 [16].

2.4. Histological analysis

The colon tissue samples fixed in the paraformaldehyde were dehydrated followed by processing of paraffin embedding, sectioning (5 μm thick) and staining (hematoxylin-eosin) and observed under light microscopy.

2.5. Colon cytokine analysis

The colonic tissues sample were fully homogenated with a homogenizer in iced-cold PBS (pH 7.4), and centrifuged at 3000 rpm for 20 min at 4 °C. The levels of tumor necrosis factor-α (TNF-α), interleukin-1β (IL-1β), and interleukin-6 (IL-6) in colons were quantified measured by using mouse enzyme-linked immunosorbent assay (ELISA) Kits (RK00027, RK00006 and RK00008, ABclonal, Wuhan, China), respectively, strictly according to the manufacturer's instruction.

2.6. Network pharmacology

2.6.1. Screening of active compounds and targets of HBHP

The chemical constituents of HBHP were obtained from the Traditional Chinese Medicine Systems Pharmacology (TCMSP, http://tcmspw.com/tcmsp.php) database and relevant research literature. The names of HBHP single-flavor Chinese medicines (Huangqin and Baishao) were used as keywords to search. The active compounds were screened by filter criteria oral bioavailability (OB) ≥ 30 % and drug-likeness (DL) ≥ 0.18 [17]. The SwissTargetPrediction database (http://www.swisstargetprediction.ch/) was used to identify potential targets for each active compound from HBHP. The only potential targets with a probability >0 were selected [18]. All targets were combined and de-duplicated for further study.

2.6.2. The acquisition of gene targets for UC

UC-related targets were collected from GeneCards (https://www.genecards.org/), GEO (https://www.ncbi.nlm.nih.gov/geo/, Series: GSE38713) and DisGeNET (https://www.disgenet.org/) databases with the keyword 'Ulcerative colitis'. The shared targets for both HBHP and UC were selected as potential therapeutic targets for HBHP against UC, and Veen diagrams were drawn.

2.6.3. Network construction

A drug-compound-target interaction network was established using Cytoscape 3.7.2 software to elucidate the relationship between herbs, active compounds and potential therapeutic targets in HBHP. NetworkAnalyzer plug-in was utilized to calculate degree, betweenness, and closeness to identify the key active compounds of HBHP in the network [19].

The potential therapeutic targets were imported into the STRING database (https://string-db.org/) to construct the protein–protein interaction (PPI) network. The combined score was set to >0.9. Then, the PPI network was visualized utilizing by Cytoscape software. CytoNCA (a Cytoscape software plugin) was employed to screen the hub genes in the network as described previously [20].

2.6.4. Gene ontology (GO) and pathway enrichment analysis

The GO function analysis and Kyoto Encyclopedia of Genes and Genomes (KEGG) pathway enrichment of the hub genes were investigated using the Database for Annotation, Visualization, and Integrated Discovery (DAVID) (https://david.ncifcrf.gov/) with the '*Homo sapiens*' setting. By consulting the literature and *P*-value rankings, the top 15 relevant GO terms and KEGG pathways were plotted as columns and bubble charts with bioinformatics platform (http://www.bioinformatics.com.cn/).

2.7. Validation of the mechanism

2.7.1. Western blot

The total protein was extracted from the colon tissues as previously reported [21]. The protein samples underwent 10 % sodium
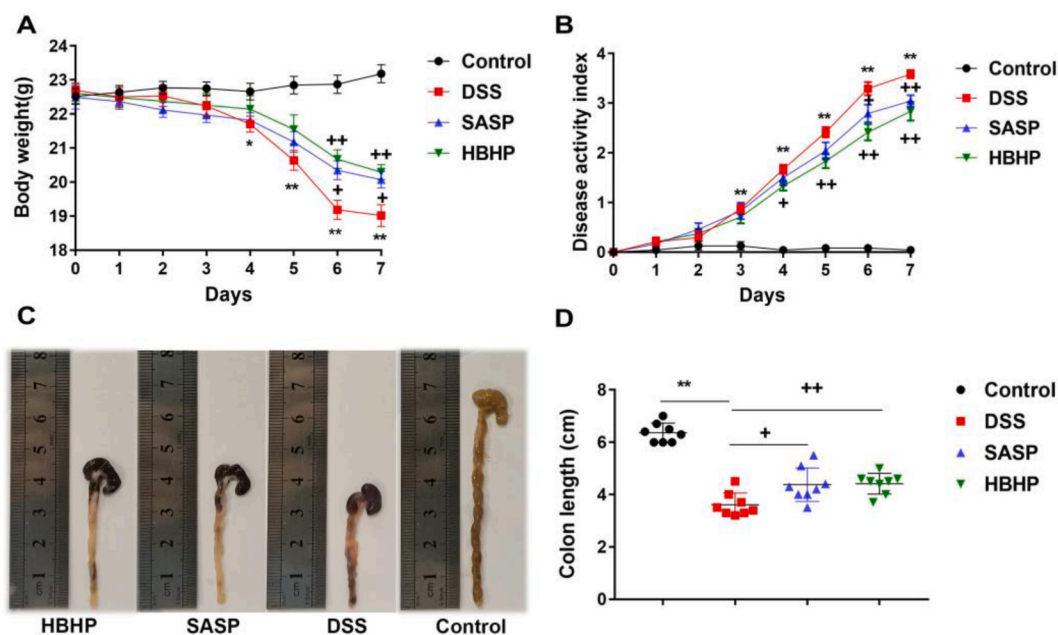
Fig. 1. HBHP alleviates DSS-induced colitis in mice. (A) Effects of the HBHP on the body weight of mice. (B) Disease activity index (DAI) score. (C) Representative images of colon. (D)Statistics of colon length. $*p < 0.05$, $**p < 0.01$ vs. the control group; $+p < 0.05$, $++p < 0.01$ vs. the DSS group.

dodecyl sulfate-polyacrylamide gel electrophoresis (SDS-PAGE) and were transferred onto polyvinylidene fluoride (PVDF) membranes in a wet transfer system. After blocking with 5 % fat-free milk for 1 h, the membranes were incubated with the following primary antibodies: anti-phospho-JAK2 (1:1000, ABclonal, AP0373), anti-phospho-STAT3 (1:1000, BOSTER, BM4835), and anti-β-Actin (1:3000, Proteintech, #66009-1-Ig) overnight at 4 °C. Following washing with tris-buffered saline with Tween 20 (TBST), the membranes were incubated with secondary antibodies (1:5000) for 30 min at room temperature. The protein bands were visualized by BeyoECL Plus (Beyotime, Shanghai, China). BioRad Quantity One software was used to analyze the results. β-Actin was used as an internal reference for semiquantitative analysis.

2.7.2. Immunohistochemistry

In brief, the paraffin sections of colon tissues were deparaffinized and rehydrated and then were treated with 0.01 M citrate buffer for antigen retrieval. The slides were treated with 3 % H_2O_2 buffer for 10 min and 5 % bovine serum albumin (BSA) for 30min, and then incubated with anti-*p*-JAK2 (#AP0531) and anti-p-STAT3 (#AP0705) (ABclonal, Wuhan, China), respectively, at a dilution of 1:100, overnight at 4 °C. After washing with PBS, the slides were incubated at 37 °C with Avidin-Biotin Complex (ABC)- horseradish peroxidase (HRP) conjugates. Diaminobenzidine was applied to shadow. Photos were taken under a microscope (BX40, Olympus, Japan).

2.7.3. Molecular docking

Molecular docking analysis was performed to demonstrate the interactions between key compounds and core targets of HBHP for treating UC and to further confirm the accuracy and reliability of the network pharmacology prediction results [22]. Structures of top-3 core compounds were downloaded from PubChem (https://pubchem.ncbi.nlm.nih.gov/). The three-dimensional (3D) structure of JAK2 (PDB ID: 5WA5) and STAT3 (PDB ID: 6DLG) was obtained from the Protein Data Bank database (http://www.rcsb.org/). Then, the Structures were converted into the pdbqt format via the AutoDockTools 1.5.6 software. Molecular docking was performed with AutoDock Vina 1.1.2 and visualized using PyMOL 2.3.2 software.

2.8. Statistical analysis

GraphPad Prism 7.0 software (San Diego, CA, United States) was used for the statistical analysis and graphics. Data were presented as the mean ± SEM. Unpaired *t*-test was used to analyze statistical comparisons between two groups. Multiple comparisons were performed by one-way ANOVA with Turkey as post-hoc tests. $p < 0.05$ was assumed as statistically significant.
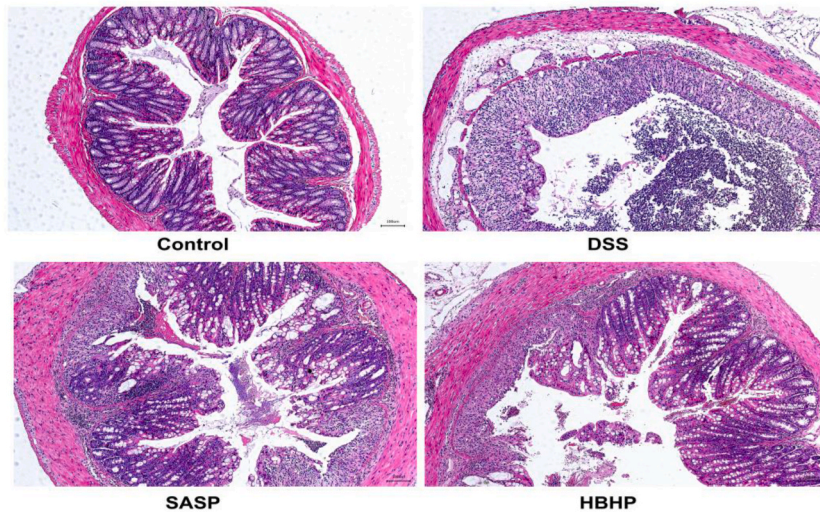
Fig. 2. Representative photomicrographs of H&E staining of colonic tissues (scale bar: 100 μm).
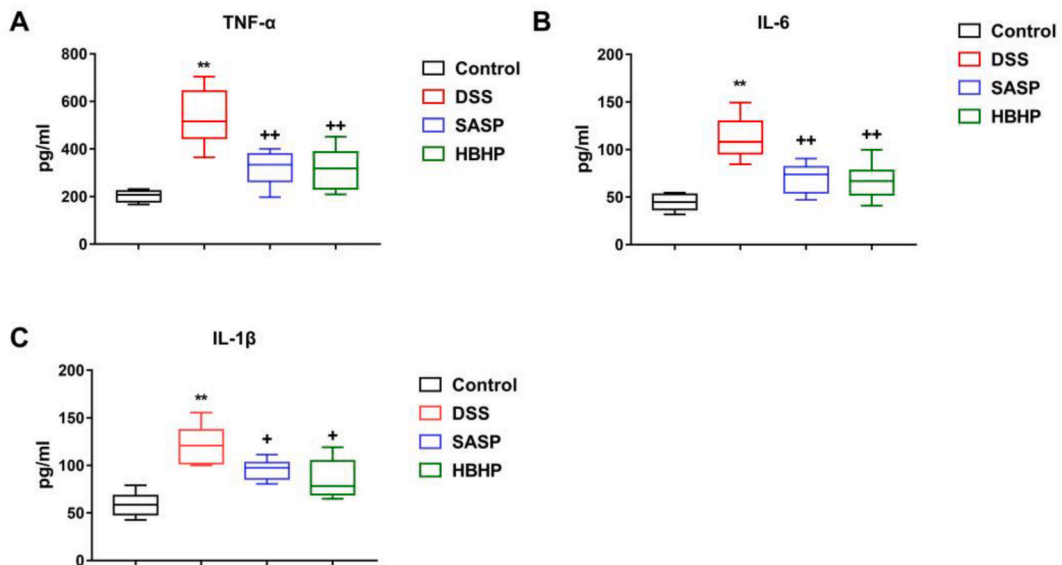

Fig. 3. Effects of HBHP on the **(A)** TNF-α, **(B)** IL-6, and **(C)** IL-1β levels in colon tissues. $*p < 0.05$, $**p < 0.01$ vs. the control group; $+p < 0.05$, $++p < 0.01$ vs. the DSS group.

3. Results

3.1. HBHP alleviated DSS-induced ulcerative colitis in mice

As shown in Fig. 1A, mice treated with DSS alone showed obvious weight loss compared to the control group, and treatment with HBHP and SASP significantly alleviated DSS-induced body weight loss ($p < 0.05$). DAI evaluation showed that DAI scores in DSS-induced mice were raised significantly ($p < 0.01$), indicating that the UC model was established successfully. After HBHP and SASP treatments, the high scores induced by DSS were markedly reversed (Fig. 1B), showing good efficacy of HBHP and SASP against UC. Furthermore, HBHP and SASP could obviously lengthen the colon of UC mice (Fig. 1C and D).

3.2. The effect of HBHP on histopathological morphology

Compared with the control group, mice in the DSS group showed severe pathological changes, such as extensive mucosal ulceration, epithelial destruction and inflammatory cell infiltration. These changes were significantly alleviated in the SASP and HBHP

Table 2
A list of the active compounds in HBHP.

No.	Mol_ID	Compound	OB(%)	DL
1	MOL001689	Acacetin	34.97	0.24
2	MOL000173	Wogonin	30.68	0.23
3	MOL002714	Baicalein	33.52	0.21
4	MOL002908	5,8,2′-Trihydroxy-7-methoxyflavone	37.01	0.27
5	MOL002910	Carthamidin	41.15	0.24
6	MOL002914	Eriodyctiol (flavanone)	48.96	0.24
7	MOL002915	Salvigenin	49.07	0.33
8	MOL002917	5,2′,6′-Trihydroxy-7,8-dimethoxyflavone	45.05	0.33
9	MOL002925	5,7,2′,6′-Tetrahydroxyflavone	37.01	0.24
10	MOL002926	Dihydrooroxylin A	38.72	0.23
11	MOL002927	Skullcapflavone II	69.51	0.44
12	MOL002928	Oroxylin a	41.37	0.23
13	MOL002932	Panicolin	76.26	0.29
14	MOL002933	5,7,4′-Trihydroxy-8-methoxyflavone	36.56	0.27
15	MOL002934	Neobaicalein	104.34	0.44
16	MOL002937	Dihydrooroxylin	66.06	0.23
17	MOL000358	Beta-sitosterol	36.91	0.75
18	MOL000359	Sitosterol	36.91	0.75
19	MOL000525	Norwogonin	39.4	0.21
20	MOL000552	5,2′-Dihydroxy-6,7,8-trimethoxyflavone	31.71	0.35
21	MOL000449	Stigmasterol	43.83	0.76
22	MOL001458	Coptisine	30.67	0.86
23	MOL001490	Bis[(2S)-2-ethylhexyl]benzene-1,2-dicarboxylate	43.59	0.35
24	MOL001506	Supraene	33.55	0.42
25	MOL002879	Diop	43.59	0.39
26	MOL002897	Epiberberine	43.09	0.78
27	MOL008206	Moslosooflavone	44.09	0.25
28	MOL010415	11,13-Eicosadienoic acid, methyl ester	39.28	0.23
29	MOL012245	5,7,4′-Trihydroxy-6-methoxyflavanone	36.63	0.27
30	MOL012246	5,7,4′-Trihydroxy-8-methoxyflavanone	74.24	0.26
31	MOL012266	Rivularin	37.94	0.37
32	MOL001919	(3S,5R,8R,9R,10S,14S)-3,17-dihydroxy-4,4,8,10,14-pentamethyl-2,3,5,6,7,9-hexahydro-1H-cyclopenta[a] phenanthrene-15,16-dione	43.56	0.53
33	MOL001924	Paeoniflorin	53.87	0.79
34	MOL000211	Mairin	55.38	0.78
35	MOL000422	Kaempferol	41.88	0.24
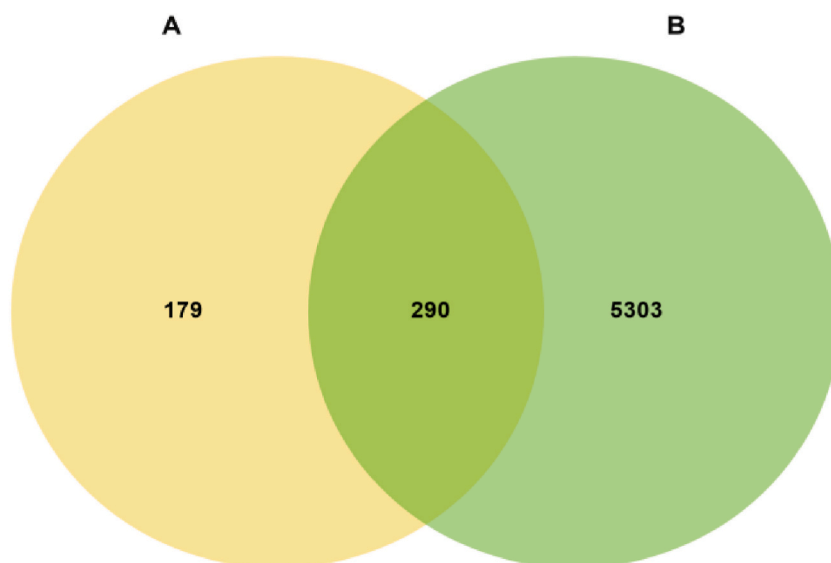
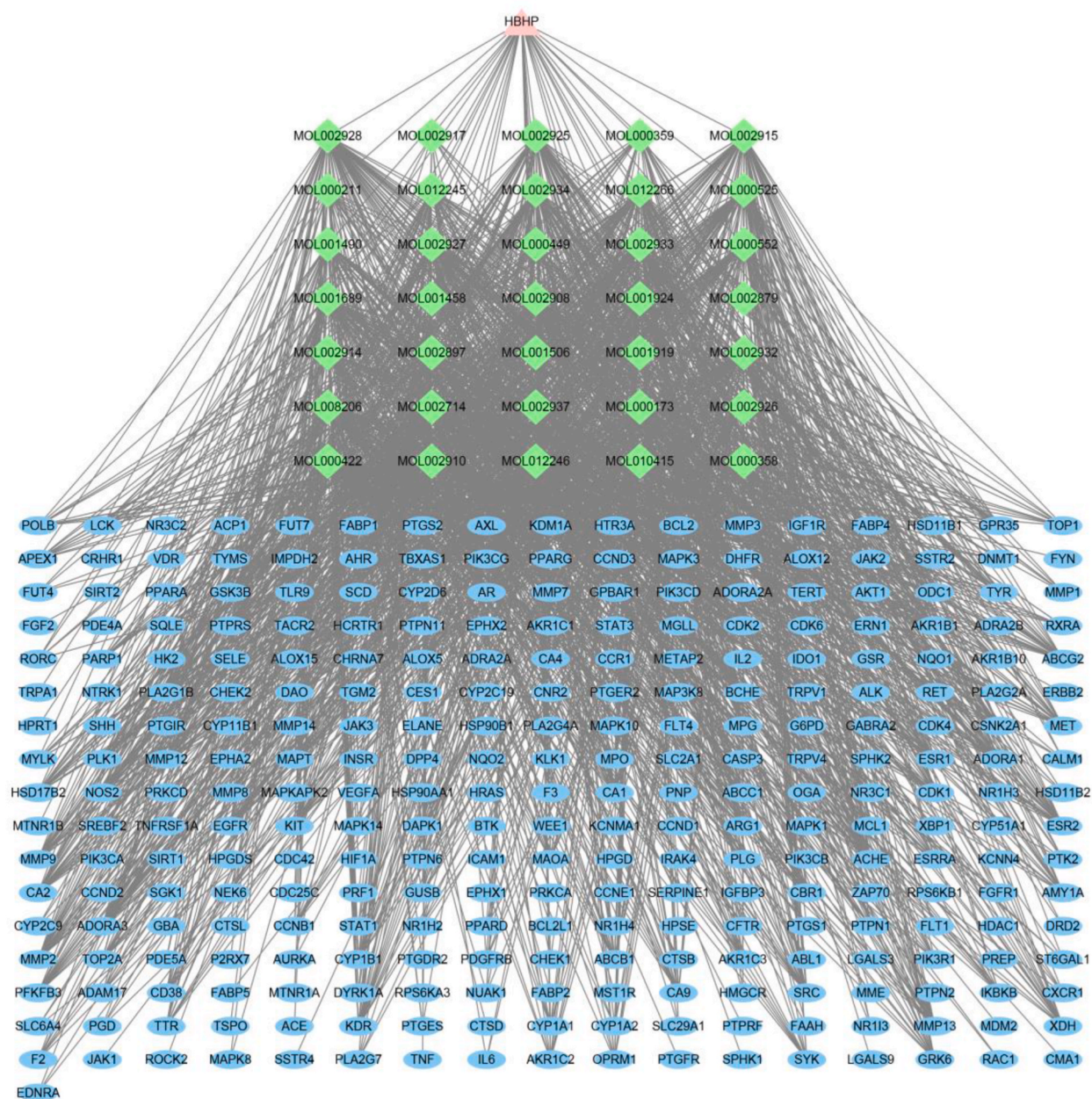**Fig. 4.** Overlapping targets between HBHP (A) and UC (B).

Fig. 5. The drug-compound-target network. Blue circles represent target proteins, green squares represent active compounds, pink triangle represents drug.

groups compared with the DSS group (Fig. 2).

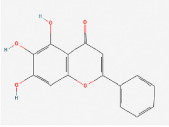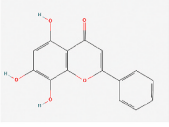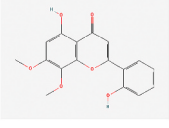### 3.3. HBHP decreased the expression of inflammatory factors

ELISA results showed TNF-α, IL-6, and IL-1β levels were markedly significantly increased in mice from the DSS group compared to the control group. However, the concentrations of TNF-α, IL-6 and IL-1β were significantly reduced by HBHP treatment (Fig. 3A–C).

3.4. Network pharmacology

3.4.1. Active compounds and potential targets of HBHP

A total of 35 compounds were obtained from TCMSP, based on OB ≥ 30 % and DL ≥ 0.18, as shown in Table 2. By fishing for targets,

Table 3
Top three compounds information of drug-compound-target network.

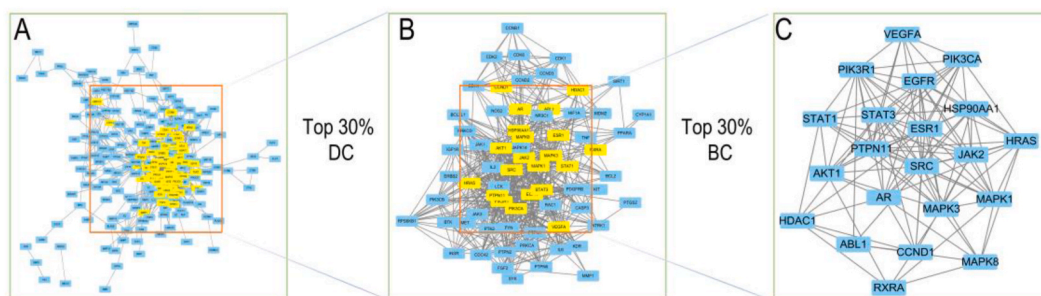| Compound	Mol_ID	Structure	Degree	Average Shortest Path Length	Betweenness Centrality	Closeness Centrality
Baicalein	MOL00271		80	2.403077	0.056046	0.416133
Norwogonin	MOL000525		79	2.409231	0.028893	0.41507
Panicolin	MOL002932		78	2.415385	0.033618	0.414013

Fig. 6. The process of identifying 21core targets (A–C).

469 potential targets were found for HBHP. Detailed information of the targets is provided in Table S1.

3.4.2. Targets of HBHP against UC

After combination and deduplication, 5593 UC-related targets were identified from the GeneCards, GEO (GSE38713) and DisGeNET. Then, the predictive targets of HBHP were overlapped with the UC-related targets. Totally, 290 potential therapeutic targets of HBHP against UC were identified for subsequent analysis. These targets are listed in Table S2 and a venn diagram was plotted (Fig. 4).

3.4.3. Network visualization

To clarify the relationship between herbs, active compounds as well as potential therapeutic targets, a drug-compound-target interaction network with 326 nodes (35 compounds, 290 target genes, and 1 herb) and 1826 edges was created by Cytoscape (Fig. 5). By analyzing this network, We discovered that baicalein, panicolin, and norwogonin were the top 3 in terms of the degree of all the active ingredients (Table 3), which may be the key active compounds for the therapeutic effects of HBHP.

The HBHP-UC target PPI network comprised 230 nodes and 1117 edges (Fig. 6A) and the sub-network was obtained by selecting the top 30 % DC, consisting of 69 nodes and 616 edges (Fig. 6B). After screening the top 30 % BC of the sub-network, the core network was finally constructed and 21 core targets were obtained (Fig. 6C).

3.4.4. GO and KEGG enrichment analysis

GO enrichment analysis demonstrated that the biological processes mainly involved positive regulation of cell migration, negative regulation of gene expression, signal transduction, etc. Cellular components mainly related to macromolecular complex, nucleoplasm, cytoplasm, etc. Molecular functions mainly included transcription factor binding, kinase activity, protein kinase binding, etc. KEGG enrichment analysis revealed that the core targets were primarily enriched in PI3K-Akt signaling pathway, Ras signaling pathway, JAK-STAT signaling pathway, etc. HBHP might act on these pathways against UC.

Table 4
The Binding energy (kcal/mol) of molecular docking simulation.

Receptors	Ligands	Binding energy (Kcal/mol)	Type of bonding	Name of residues	Ligand atoms
5WA5 (JAK2)	Baicalein	−9.1	Hydrogen Bonds	ASN140	O(4), H(1051)
			Hydrophobic Interactions	PRO82	O(445), O(7)
			Hydrogen Bonds	MET105	O(672), H(231)
	Panicolin	−8	Hydrogen Bonds	ASN140	O(8), H(1053)
			Hydrogen Bonds	ASN140	O(22), H(1053)
			Hydrophobic Interactions	PRO82	O(447), O(11)
			Hydrophobic Interactions	PRO82	O(447), O(20)
			Hydrophobic Interactions	MET132	O(961), C(25)
	Norwogonin	−8.5	Hydrogen Bonds	ASN140	O(4), H(1051)
			Hydrogen Bonds	ASN140	O(20), H(1051)
			Hydrophobic Interactions	PRO82	O(445), O(7)
			Hydrogen Bonds	MET132	O(959), H(23)
6DLG (STAT3)	Baicalein	−9	Hydrogen Bonds	HIS635	N(2035), H(23)
			Hydrophobic Interactions	HIS635	N(2035), O(20)
			Hydrogen Bonds	PHE636	O(2048), H(21)
			Hydrophobic Interactions	PHE636	N(2045), O(20)
	Panicolin	−8.6	Hydrogen Bonds	ARG581	O(1528), H(19)
			Hydrophobic Interactions	SER537	O(1141), O(20)
			Hydrophobic Interactions	THR583	O(1552), O(20)
	Norwogonin	−9.6	Hydrogen Bonds	SER537	O(1139), H(19)
			Hydrophobic Interactions	SER537	N(1130), O(19)
			Hydrophobic Interactions	SER758	N(978), O(20)

3.5. Preliminary verification of the mechanism of HBHP on UC

3.5.1. HBHP down-regulated expression of p-JAK2 and p-STAT3 proteins

The expression levels of JAK2 and STAT3 proteins in colon tissues were investigated via Western blot (Fig. 8A) and immunohistochemistry (Fig. 8B). As shown in Fig. 8A, the protein expression of JAK and STAT3 was significantly increased in the DSS group compared with that in the control group, while HBHP and SASP treatment inhibited the increase. The results of immunohistochemistry were consistent with those of Western blot.

3.5.2. Molecular docking

Binding energies < -5.0 kcal/mol indicate good binding activity [23,24]. Our results suggested that the key compounds and core targets (JAK2, STAT3) had good binding interactions and the detailed affinity was shown in Table 4, reflecting that the key active compounds of HBHP could treat UC through JAK2 and STAT3. The docking mode diagrams of core targets-key active compounds were displayed in Fig. 9.

Baicalein-STAT3. (B1) Panicolin-JAK2. (B2) Panicolin-STAT3. (C1) Norwogonin- JAK2. (C2).

4. Discussion

UC is a chronic, idiopathic inflammatory disease whose exact pathogenesis is not yet fully understood [25]and the available remedies are not satisfactory [26]. Common clinical symptoms of UC are bloody stool, diarrhea and weight loss. According to pathogenesis and clinical manifestations, UC is classified into the categories of "dysentery", "diarrhea" and "hematochezia" recorded in TCM [8]. TCM, with lower adverse effects [27], has been widely used to treat UC in China [28]. The combination use of huangqin and baishao with the ratio of 3:2 was first proposed by Zhongjing Zhang (in Eastern Han Dynasty) in the treatise "Shang Han Lun" and HBHP has been used clinically to treat gastrointestinal diseases such as UC for nearly 1800 years in China. Given the specificity of multi-component, multi-target and multi-channel Chinese herbal formulations, the potential molecular mechanisms of HBHP against UC remain unclear and need further study.

In this study, we used an in vivo experimental–network pharmacology–experimental validation approach to investigate the protective effect efficacy and potential mechanisms of HBHP in the treatment of UC. Here, a mouse UC model was induced by DSS. Consistent with previous studies [14,21], during the construction of the model, the mice experienced weight loss, gradually increased diarrhea with bloody stools. Our study confirmed that HBHP could effectively alleviate signs and symptoms of DSS-induced UC in mice, including weight loss and elevated DAI scores. Colon shortening is an important characteristic of DSS-induced UC, and HBHP significantly reversed the change ($p < 0.01$). In addition, HBHP could attenuates colonic pathological damage including inflammatory cell infiltration and reduce the levels of inflammatory cytokines in colon tissues of UC mice ($p < 0.05$ or $p < 0.01$), indicating that HBHP inhibited the inflammatory response of UC to a certain extent. TNF-α, IL-6, and IL-1β are involved in the pathological processes associated with UC [1,29]. During the process of UC, the release of inflammatory mediators (TNF-α, IL-1β, IL-6, etc) will intensify the infiltration of inflammatory cells in colon tissue, trigger inflammatory response and further destroy intestinal mucosal, which would lead to the formation of ulceration. These results demonstrated that HBHP has a positive therapeutic effect on DSS-induced UC.

Subsequently, we used network pharmacology method to predict the potential mechanism of action of HBHP in UC. Upon strict
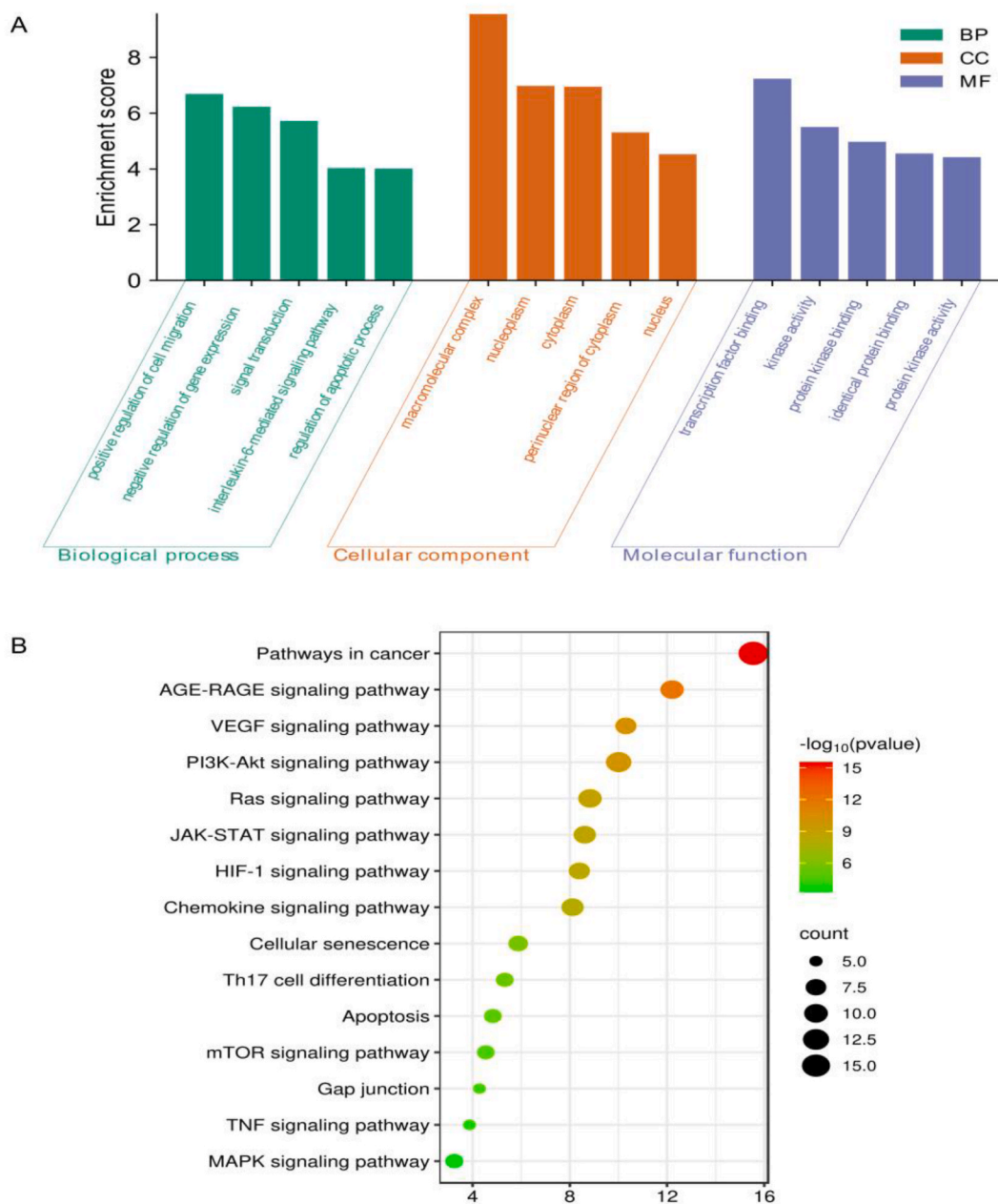
Fig. 7. GO (A) and KEGG (B) enrichment results of core targets. The size of each dot indicates gene count. The color of circles represents different -log10 (p-value).

screening, we obtained 35 active compounds from HBHP that acted on 290 targets of UC. The network topology analysis suggested that baicalin, norwogonin and panicolin might be the main components of HBHP in the treatment of UC. According to previous reports, baicalein could not only alleviate symptoms of UC mice induced by DSS and improve murine colonic histological structure [30], but also down-regulate levels of inflammatory cytokines (IL-17, IL-6, and TNF-α) in serum [31]. Panicolin also known as skullcapflavone I (a flavonoid) significantly inhibited LPS-induced IL-6 production in a concentration-dependent manner and showed anti-inflammatory effects [32]. A Study had revealed that the anti-complementary active metabolites of the aqueous extract of Scutellaria baicalensis roots were identified as norwogonin, baicalein, and oroxylin A, among which norwogonin was the most active compound [33]. In summary, it is reliable and feasible to use network pharmacology to search for potentially active compounds.

The PPI and enrichment results revealed that the core targets of HBHP in the treatment of UC may be STAT3, JAK2, SRC, PIK3CA, VEGFA, etc., and these targets are mainly mapped to key pathways such as the VEGF signaling pathway, PI3K-Akt signaling pathway and JAK-STAT signaling pathway and other pathways by intervening in biological processes such as cell proliferation and apoptosis
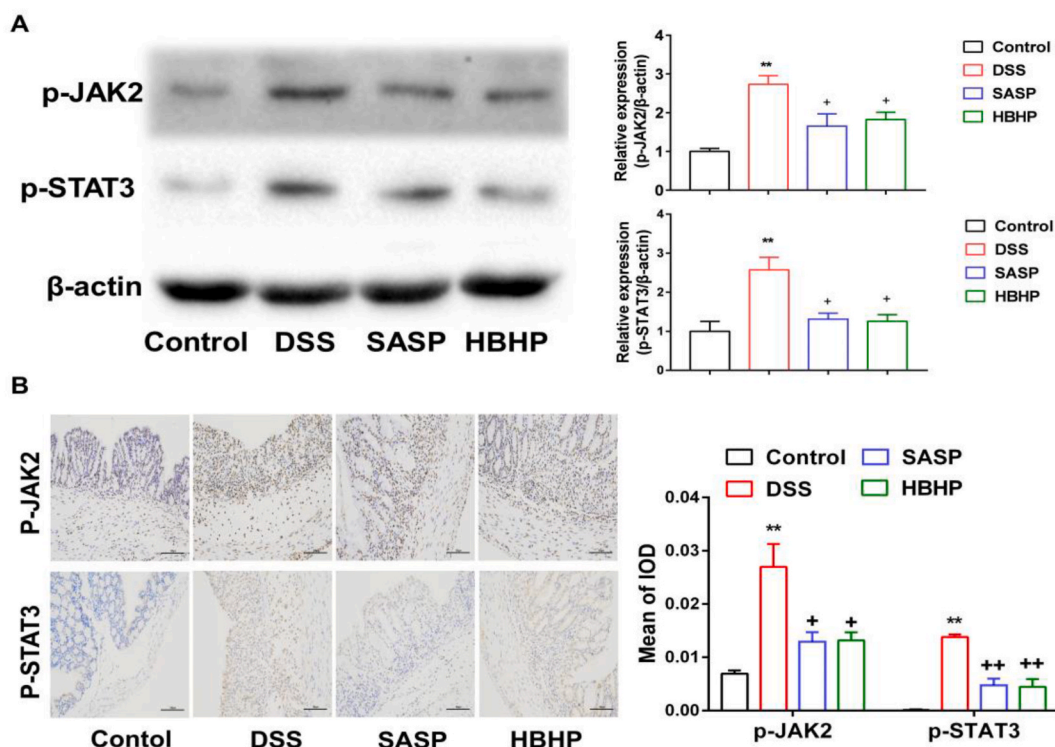
Fig. 8. Effects of HBHP on *p*-JAK2 and p-STAT3 expression in colon tissues by Western blot (A) analysis or immunochemistry (B). **$p < 0.01$ vs. the control group; $+p < 0.05$, $++p < 0.01$ vs. the DSS group.

and estrogen response regulation (shown in Fig. 7). Currently, there is a lot of evidence linking JAK/STAT signaling pathway to the pathogenesis of UC. Inflammation is crucial for the occurrence of UC [34]. It's been reported that the JAK/STAT axis is implicated inflammation [35,36]. Numerous cytokines affect JAK/STAT signaling. JAKs such as JAK1, JAK2, TYK2 and JAK3 bind non-covalently to different cytokine receptors, and mediate receptors tyrosine phosphorylation, and then recruit ≥1 STAT proteins such as STAT1, STAT2, STAT3 and STAT4, etc [35]. STATs undergo phosphorylation and dimerize. The active STATs are then transported into the nucleus and act as transcription factors to modulate downstream genes expression [37]. The JAK2/STAT3 pathway is widely accepted as a classical and major inflammatory pathway. Abnormal activation of the JAK2/STAT3 pathway is closely associated with the progression of many inflammatory diseases, including UC [38]. Overactivation of the JAK2/STAT3 signaling pathway may have a negative impact on UC [39]. Elevated JAK2 mRNA and protein expression have been reported in UC patients [40,41]. Levels of phosphorylated STAT3 was increased in pediatric patients with UC [42] and positively correlated with disease severity [43]. It is well established that activation of the JAK2/STAT3 pathway is achieved through IL-6, which has been shown to be positively correlated with the development of UC [44]. IL6 binds to its receptor complex IL6R-gp130 and activates downstream JAK2, which then activate STAT3 through phosphorylation of Tyrosine 705. Phosphorylated STAT3 subsequently activate the nuclear transcription factor NF-κB, which move into the nucleus and then regulates the expression of inflammatory cytokines [45]. A previous study showed that sphk1 promotes ulcerative colitis via activating JAK2/STAT3 signaling pathway. *Rubia cordifolia* L. could ameliorate DSS-induced ulcerative colitis in mice by inhibiting IL-6/JAK2/STAT3 pathway. Based on network pharmacology and literature analysis, the underlying mechanism of HBHP against UC appears to be strongly related to JAK2/STAT3 pathway. Therefore, the protein levels of phosphorylated-JAK2 and phosphorylated-STAT3 were further detected by WB and IHC. Upregulated JAK2 and STAT3 expressions were detected in colonic tissue in the DSS group mice, which is consistent with previous documents [46,47]; however, both of them were significantly reduced with HBHP treatment ($p < 0.05$ or $p < 0.01$). Molecular docking results suggested that the main active compounds of HBHP exhibited strong binding interactions with JAK2 and STAT3 (affinity < −8.00 kcal/mol). Moreover, these findings were accompanied by reduced inflammatory cytokinesand improved pathological changes, indicating that suppression of the inflammatory response and affecting the JAK2/STAT3 signaling pathway were at least in part responsible for HBHP exerting its anti-UC efficacy. However, the speculation should be supported and validated by further basic and clinical experimental data.

5. Conclusion

HBHP could alleviate DSS-induced ulcerative colitis, and its mechanism might primarily be achieved by downregulating JAK2 and STAT3 expression in colonic tissue to reduce inflammation via JAK2/STAT3 pathway. These findings have provided new evidence that HBHP might play an important role in UC treatment and further molecular mechanism studies of HBHP in treating UC deserve study.
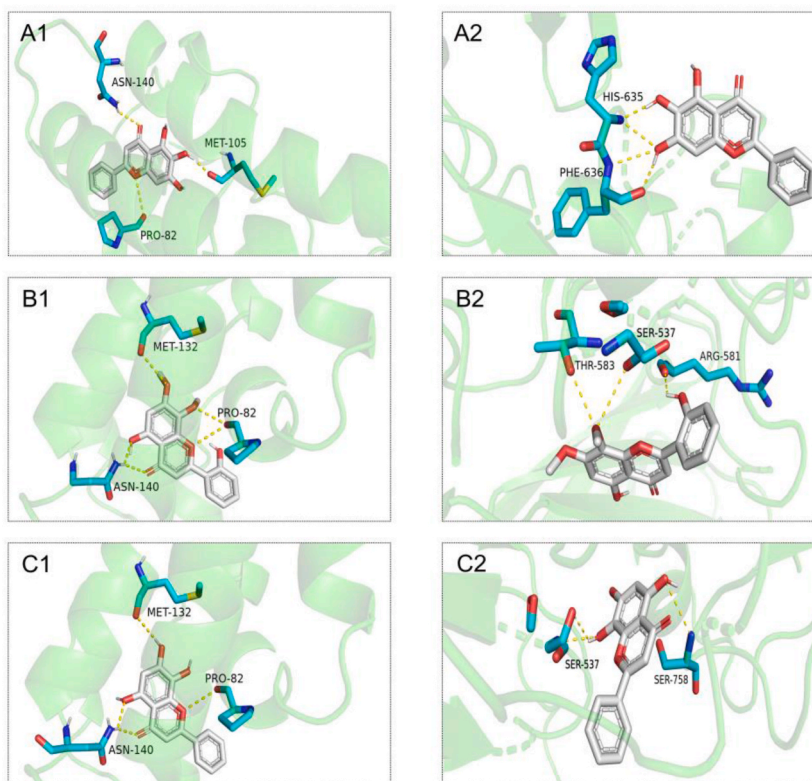
Fig. 9. Docking patterns of representative receptor ligand pairs. (A1) Baicalein- JAK2. (A2).

5.1. Limitation

HBHP is a traditional Chinese medicine formula that treats UC through multiple targets and multiple pathways. We just focused on the classical JAK2/STAT3 pathway, rather than other pathways such as HIF-1 pathway and mTOR pathway, etc. In addition, the predicted synergistic effects between multi-components, multi-targets and multi-signaling pathways have not been further analyzed. Consequently, further research is needed to provide a more accurate basis for the predictive results of this study.

Funding statement

Data availability statement

The datasets used and analyzed in this study are available from the corresponding author upon request.

CRediT authorship contribution statement

Bailu Duan: Writing – original draft, Data curation, Validation. **Qiong Hu:** Data curation. **Fengmin Ding:** Investigation. **Fang Huang:** Data curation. **Wei Wang:** Investigation. **Nina Yin:** Investigation. **Zhe Liu:** Investigation. **Song Zhang:** Investigation. **Dongchu He:** Conceptualization. **Qiping Lu:** Conceptualization.

Declaration of competing interest

The authors declare that they have no known competing financial interests or personal relationships that could have appeared to influence the work reported in this paper.

Appendix A. Supplementary data

Supplementary data to this article can be found online at https://doi.org/10.1016/j.heliyon.2023.e23082.

References

[1] H. Nakase, et al., The influence of cytokines on the complex pathology of ulcerative colitis, Autoimmun. Rev. 21 (3) (2022), 103017.
[2] J.P. Segal, J.F. LeBlanc, A.L. Hart, Ulcerative colitis: an update, Clin. Med. 21 (2) (2021) 135–139.
[3] J. Chen, et al., Bidirectional mendelian randomisation analysis provides evidence for the causal involvement of dysregulation of CXCL9, CCL11 and CASP8 in the pathogenesis of ulcerative colitis, Journal of Crohns & Colitis 17 (5) (2023) 777–785.
[4] G.G. Kaplan, J.W. Windsor, The four epidemiological stages in the global evolution of inflammatory bowel disease, Nat. Rev. Gastroenterol. Hepatol. 18 (1) (2021) 56–66.
[5] L. Zhang, et al., Colon tissue-accumulating mesoporous carbon nanoparticles loaded with Musca domestica cecropin for ulcerative colitis therapy, Theranostics 11 (7) (2021) 3417–3438.
[6] S.E. Berends, et al., Clinical pharmacokinetic and pharmacodynamic considerations in the treatment of ulcerative colitis, Clin. Pharmacokinet. 58 (1) (2019) 15–37.
[7] Y.T. Niu, et al., Glycosides as potential medicinal components for ulcerative colitis: a review, Molecules 28 (13) (2023).
[8] J. Chen, B.X. Shen, Z.L. Jiang, Traditional Chinese medicine prescription Shenling BaiZhu powder to treat ulcerative colitis: clinical evidence and potential mechanisms, Front. Pharmacol. 13 (2022).
[9] R. Wang, et al., Saponins in Chinese herbal medicine exerts protection in myocardial ischemia-reperfusion injury: possible mechanism and target analysis, Front. Pharmacol. 11 (2020), 570867.
[10] N. Zhang, et al., Neutrophil degranulation and myocardial infarction, Cell Commun. Signal. 20 (1) (2022) 50.
[11] E. Yague, H. Sun, Y. Hu, East wind, west wind: toward the modernization of traditional Chinese medicine, Front. Neurosci. 16 (2022), 1057817.
[12] R.Z. Zhang, et al., Network pharmacology databases for traditional Chinese medicine: review and assessment, Front. Pharmacol. 10 (2019).
[13] W. Zhang, et al., Network pharmacology and in vitro experimental verification to explore the mechanism of Sanhua decoction in the treatment of ischaemic stroke, Pharm. Biol. 60 (1) (2022) 119–130.
[14] Y.L. Chen, et al., Systems pharmacology approach reveals the antiinflammatory effects of Ampelopsis grossedentata on dextran sodium sulfate-induced colitis, World J. Gastroenterol. 24 (13) (2018) 1398–1409.
[15] H. Zhuang, et al., Tiliroside ameliorates ulcerative colitis by restoring the M1/M2 macrophage balance via the HIF-1alpha/glycolysis pathway, Front. Immunol. 12 (2021), 649463.
[16] S.S. Gong, et al., Mucosa repair mechanisms of Tong-Xie-Yao-Fang mediated by CRH-R2 in murine, dextran sulfate sodium-induced colitis, World J. Gastroenterol. 24 (16) (2018) 1766–1778.
[17] Y. Cao, et al., Network pharmacology and experimental validation to explore the molecular mechanisms of Bushen Huoxue for the treatment of premature ovarian insufficiency, Bioengineered 12 (2) (2021) 10345–10362.
[18] S.A. Khan, T.K.W. Lee, Network pharmacology and molecular docking-based investigations of Kochiae Fructus's active phytomolecules, molecular targets, and pathways in treating COVID-19, Front. Microbiol. 13 (2022).
[19] S.H. Feng, et al., Danggui buxue decoction in the treatment of metastatic colon cancer: network pharmacology analysis and experimental validation, Drug Des. Dev. Ther. 15 (2021) 705–720.
[20] J. Jin, et al., Network pharmacology and molecular docking study on the mechanism of colorectal cancer treatment using Xiao-Chai-Hu-Tang, PLoS One 16 (6) (2021), e0252508.
[21] L. Peng, et al., Astragalin attenuates dextran sulfate sodium (DSS)-Induced acute experimental colitis by alleviating gut microbiota dysbiosis and inhibiting NF-kappa B activation in mice, Front. Immunol. 11 (2020).
[22] H. Tong, et al., Bioactive constituents and the molecular mechanism of Curcumae Rhizoma in the treatment of primary dysmenorrhea based on network pharmacology and molecular docking, Phytomedicine 86 (2021), 153558.
[23] X. Li, et al., Network pharmacology prediction and molecular docking-based strategy to explore the potential mechanism of Huanglian Jiedu Decoction against sepsis, Comput. Biol. Med. (2022) 144.
[24] S.D. Long, et al., Network pharmacology and molecular docking analysis reveal insights into the molecular mechanism of shiliao decoction in the treatment of cancer-associated malnutrition, Front. Nutr. 9 (2022).
[25] T. Zhang, et al., Research trends in ulcerative colitis: a bibliometric and visualized study from 2011 to 2021, Front. Pharmacol. 13 (2022), 951004.
[26] B. Zeng, et al., ILC3 function as a double-edged sword in inflammatory bowel diseases, Cell Death Dis. 10 (4) (2019) 315.
[27] I. Khan, et al., Alteration of gut microbiota in inflammatory bowel disease (IBD): cause or consequence? IBD treatment targeting the gut microbiome, Pathogens 8 (3) (2019).
[28] F.S. Kou, et al., Clinical evaluation of traditional Chinese medicine on mild active ulcerative colitis: a multi-center, randomized, double-blind, controlled trial, Medicine (Baltim.) 99 (35) (2020), e21903.
[29] H. Hanai, Positions of selective leukocytapheresis in the medical therapy of ulcerative colitis, World J. Gastroenterol. 12 (47) (2006) 7568–7577.
[30] C. Liu, et al., Baicalein Restores the Balance of Th17/Treg Cells via Aryl Hydrocarbon Receptor to Attenuate Colitis, vol. 2020, Mediators Inflamm, 2020, 5918587.
[31] S. Liang, et al., The comparative study of the therapeutic effects and mechanism of baicalin, baicalein, and their combination on ulcerative colitis rat, Front. Pharmacol. 10 (2019) 1466.
[32] C.V. Chandrasekaran, et al., In vitro modulation of LPS/calcimycin induced inflammatory and allergic mediators by pure compounds of Andrographis paniculata (King of bitters) extract, Int. Immunopharm. 11 (1) (2011) 79–84.
[33] S. Xing, et al., Simulated gastrointestinal tract metabolism and pharmacological activities of water extract of Scutellaria baicalensis roots, J. Ethnopharmacol. 152 (1) (2014) 183–189.
[34] T. Kobayashi, et al., Ulcerative colitis, Nat. Rev. Dis. Prim. 6 (1) (2020) 74.
[35] R.P. Agashe, S.M. Lippman, R. Kurzrock, JAK: not just another kinase, Mol. Cancer Therapeut. 21 (12) (2022) 1757–1764.
[36] S. Banerjee, et al., JAK-STAT signaling as a target for inflammatory and autoimmune diseases: current and future prospects, Drugs 77 (5) (2017) 521–546.
[37] K.L. Owen, N.K. Brockwell, B.S. Parker, JAK-STAT signaling: a double-edged sword of immune regulation and cancer progression, Cancers 11 (12) (2019).
[38] A.M. Chen, et al., Matrine protects colon mucosal epithelial cells against inflammation and apoptosis via the Janus kinase 2/signal transducer and activator of transcription 3 pathway, Bioengineered 13 (3) (2022) 6490–6499.
[39] Z. Lu, et al., Huanglian Jiedu Decoction ameliorates DSS-induced colitis in mice via the JAK2/STAT3 signalling pathway, Chin. Med. 15 (1) (2020).
[40] M. Hedl, D.D. Proctor, C. Abraham, JAK2 disease-risk variants are gain of function and JAK signaling threshold determines innate receptor-induced proinflammatory cytokine secretion in macrophages, J. Immunol. 197 (9) (2016) 3695–3704.
[41] L. Song, et al., High intestinal and systemic levels of interleukin-23/T-helper 17 pathway in Chinese patients with inflammatory bowel disease, Mediat. Inflamm. 2013 (2013), 425915.

[42] G. Koukos, et al., MicroRNA-124 regulates STAT3 expression and is down-regulated in colon tissues of pediatric patients with ulcerative colitis, Gastroenterology 145 (4) (2013) 842–852 e2.

[43] R. Carey, et al., Activation of an IL-6:STAT3-dependent transcriptome in pediatric-onset inflammatory bowel disease, Inflamm. Bowel Dis. 14 (4) (2008) 446–457.

[44] Y. Li, et al., IL-6/STAT3 signaling pathway regulates the proliferation and damage of intestinal epithelial cells in patients with ulcerative colitis via H3K27ac, Exp. Ther. Med. 22 (2) (2021) 890.

[45] W. Qin, et al., Rubia cordifolia L. ameliorates DSS-induced ulcerative colitis in mice through dual inhibition of NLRP3 inflammasome and IL-6/JAK2/STAT3 pathways, Heliyon 8 (8) (2022), e10314.

[46] Y. Zhao, et al., Gegen Qinlian decoction relieved DSS-induced ulcerative colitis in mice by modulating Th17/Treg cell homeostasis via suppressing IL-6/JAK2/STAT3 signaling, Phytomedicine 84 (2021), 153519.

[47] J. Wang, et al., TAK-242 ameliorates DSS-induced colitis by regulating the gut microbiota and the JAK2/STAT3 signaling pathway, Microb. Cell Factories 19 (1) (2020) 158.